Dynamic Article Links ▶

PAPER

Discovering potent inhibitors against c-Met kinase: molecular design, organic synthesis and bioassay†

Zhongjie Liang,‡[a] Xiao Ding,‡[a] Jing Ai,‡[b] Xiangqian Kong,[a] Limin Chen,[a] Liang Chen,[a] Cheng Luo,*[a,c] Meiyu Geng,*[b] Hong Liu,*[a] Kaixian Chen[a] and Hualiang Jiang[a]

The receptor tyrosine kinase c-Met is an attractive target for therapeutic treatment of cancers nowadays. The discovery of small molecule inhibitors is of special interest in the blockade of the c-Met kinase pathway. Here, we initiated our study from compound **1a**, a novel inhibitor against c-Met kinase. A substructure similarity search against the SPECS database and chemical synthesis methods were performed to obtain a series of pyrazolidine-3,5-dione derivatives. Through the enzyme-based assay against c-Met kinase, 4 compounds (**1c**, **1e**, **1m** and **1o**) showed potential inhibitory activity, with IC_{50} values mostly less than 10 μM. Based on the structure–activity relationship (SAR) and binding mode analysis, a focused combinatorial library was designed by the LD1.0 program. Taking into account ADMET properties and synthesis accessibility, seven candidate compounds (**5a–g**) were successfully synthesized. The activity of the most potent compounds **5b** (IC_{50} = 0.46 μM) was 20 fold higher than that of the lead **1a**. Taken together, our findings identified the pyrazolidine-3,5-dione derivatives as potent inhibitors against c-Met kinase and demonstrated the efficiency of the strategy in the development of small molecules against c-Met kinase.

Introduction

c-Met kinase, which is encoded by proto-oncogene MET (mesenchymal-epithelial transition factor), is the cell-surface receptor for hepatocyte growth factor (HGF). The kinase, together with its natural ligand HGF, is an important paracrine mediator of epithelial-mesenchymal cell interactions involved in the regulation of multiple cellular activities, including cell migration, mitogenesis, morphogenesis, and angiogenesis.[1] The kinase activation is consequently essential for embryonic development and wound healing.[2] Moreover, c-Met kinase can be over-activated *via* a variety of mechanisms, including ligand-dependent activation (autocrine or paracrine), gene amplification, gene mutation and cross-talk with other receptors (heterodimerization).[3] The activation gives rise to receptor dimerization and recruitment of several SH2 domain-containing signal transducers that activate a number of pathways including the GRB2-SOS-RAS-RAF-MEK-ERK axis,

PI3K-AKT-mTOR cascade and so on.[2] When deregulated, the over activation of the kinase has been implicated in tumor cell proliferation, angiogenesis, invasion/metastasis and resistance to apoptosis and cytotoxic therapies, which implied the kinase as an attractive therapeutic target.[4] Consequently, inhibiting the HGF/c-Met kinase pathway would have potent anti-tumor effects *via* multiple complementary mechanisms. To date, numerous examples of successful therapeutic interventions with c-Met kinase inhibitors have been reported, which in turn has proved the kinase as a target of priority.[5–9]

Nowadays, several different strategies targeting the HGF/c-Met kinase pathway have been explored,[1,5] each focusing on one of the serial steps that regulate c-Met kinase activation. The strategies include: (a) blocking the interaction between c-Met kinase and HGF by antagonists or neutralizing antibodies, such as NK1 and NK2 isoforms,[10,11] (b) blocking the phosphorylation of tyrosine residues in the kinase domain by small molecule inhibitors which compete for ATP binding at the active site, and (c) blocking the c-Met kinase dependent signaling by interfering with c-Met associated signal transducers or downstream signaling components.[12] Amongst these strategies, inhibition of the kinase activity by small molecules is a pharmacologically attractive method that has been demonstrated for other tyrosine kinases.[13]

Recently, we identified compound (**1a**) from screening of our in-house SPECS database as an inhibitor against c-Met kinase with an IC_{50} value of 9.5 μM. By virtue of the cost-inefficient and time-consuming process of conventional drug discovery over decades, focused combinatorial library design has been proved to be a

[a] Drug Discovery and Design Center, State Key Laboratory of Drug Research, Shanghai Institute of Materia Medica, Chinese Academy of Sciences, Shanghai, 201203, China. E-mail: hliu@mail.shcnc.ac.cn; Fax: +86-21-50807188; Tel: +86-21-50806600

[b] Division of Anti-Tumor Pharmacology, State Key Laboratory of Drug Research, Shanghai Institute of Materia Medica, Chinese Academy of Sciences, Shanghai, 201203, China. E-mail: mygeng@mail.shcnc.ac.cn

[c] Center for Systems Biology, Soochow University, Jiangsu, 215006, China. E-mail: cluo@mail.shcnc.ac.cn

† Electronic supplementary information (ESI) available. See DOI: 10.1039/c1ob06186k

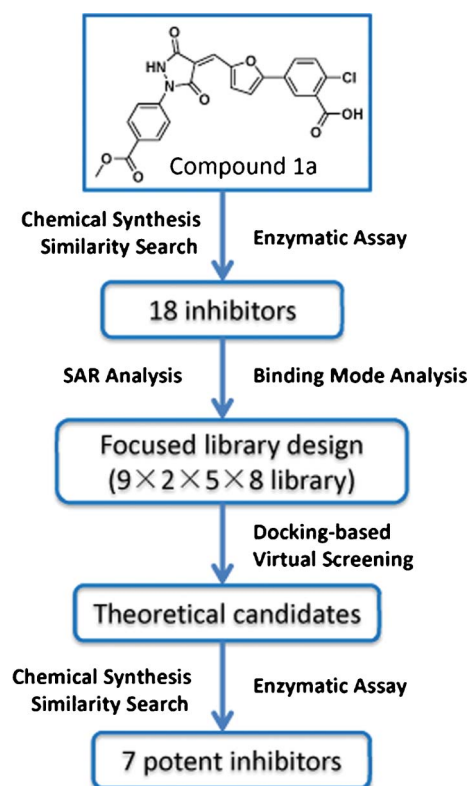‡ These authors contributed equally to this study.

This journal is © The Royal Society of Chemistry 2012

Org. Biomol. Chem., 2012, **10**, 421–430 | 421

Fig. 1 Flow chart of the discovery strategy for c-Met kinase inhibitors in this study.

complementary method in rational drug design.[14] Here we present a structure based molecular design to identify the pyrazolidine-3,5-dione derivatives as potent c-Met kinase inhibitors. Firstly, we performed a substructure similarity search against the SPECS database on the pyrazolidine-3,5-dione scaffold. Meanwhile, the chemical synthesis method was also employed. After evaluating for their inhibitory activity by *in vitro* enzymatic assay, 18 compounds (including **1a**) were identified as inhibitors against c-Met kinase. In addition, among them, 4 compounds (**1c**, **1e**, **1m** and **1o**) showed moderate potency, with IC$_{50}$ values less than 10 μM. Secondly, based on the structure–activity relationship (SAR) and analysis of their binding modes compared with X-ray crystal structures, fragments of advantage were extracted for the design of a focused combinatorial library containing 720 molecules by the LD1.0 program. Taking into account the ADMET properties and feasibility of chemical synthesis, seven compounds (**5a–g**) were successfully synthesized ultimately. The activity of the most potent compounds **5b** (IC$_{50}$ = 0.46 μM) was ~20 fold higher than that of the lead compound **1a**. The detailed design procedure is shown in Fig. 1. Overall, our study demonstrated that the pyrazolidine-3,5-dione could be a better lead scaffold for c-Met kinase inhibitors, which will accelerate the discovery of new inhibitors against c-Met kinase.

Results and discussion

Identification of pyrazolidine-3,5-dione derivatives as c-Met kinase inhibitors

Compound **1a** from our in-house database was identified as an inhibitor against c-Met kinase, with an IC$_{50}$ value of 9.5 μM.

To further develop better inhibitors based on this scaffold, a substructure similarity search against the SPECS database and chemical synthesis were performed on the pyrazolidine-3,5-dione scaffold. By *in vitro* assay against c-Met kinase, 18 compounds (**1a–r**) stand out as c-Met kinase inhibitors, whose structures are shown in Table 1. The compounds labeled with asterisks were synthesized through the routes outlined in Scheme 1, and the details of the synthetic procedures and structural characterizations are described in the Experimental section. The primary inhibitory activities of these compounds at 10 μM against c-Met kinase were determined, and IC$_{50}$ values were measured for the compounds with better inhibitory activities (>50%), which are also listed in Table 1. The detail bioassay protocol is described in the Experimental section.

SAR analysis indicated that substituent R$_2$ of the A ring was essential for the inhibitory activity against c-Met kinase. Among these derivatives, esters proved to be the favored substituent for the R$_2$ group (**1a–1c**). Replacing the ester group with a methyl group (**1a** and **1d–1e**), a methoxy group (**1a** and **1f**) or a nitro group (**1a** and **1g**) actually reduced the enzyme potency to 48.1%, 23.6% and 43.2%, respectively. The removal of the ester groups made the compounds basically lose the inhibitory activity (**1a** and **1j**). Furthermore, H-bond donating groups on R$_5$ or R$_6$ of the D ring were also essential for the inhibitory activities. Consequently, a carboxyl group and an ester group (**1a–1e**, **1h–1i**) on R$_6$ afforded good enzyme potency. Replacing R$_6$ with a chloro group decreased the inhibitory activity (**1b** and **1k**) and the change of the chloro group to R$_4$ also decreased the activity (**1k** and **1l**). The introduction of the H-bond donating group sulfamide to R$_5$ afforded compounds **1m**, **1n** and **1o** with inhibition of 56.2%, 43.4% 57.6%, respectively. In addition, replacing the furan ring (C ring) with a benzene ring weakened the inhibitory activity to 42.2% (**1c** and **1p**). It is also worth noting that the inhibitory activities were abolished when the pyrazolidine-3,5-dione ring was replaced by a 3-methyl-1*H*-pyrazol-5(4*H*)-one ring (**1p** and **1q**) or a 3-ethoxy-1*H*-pyrazol-5(4*H*)-one ring (**1b** and **1r**).
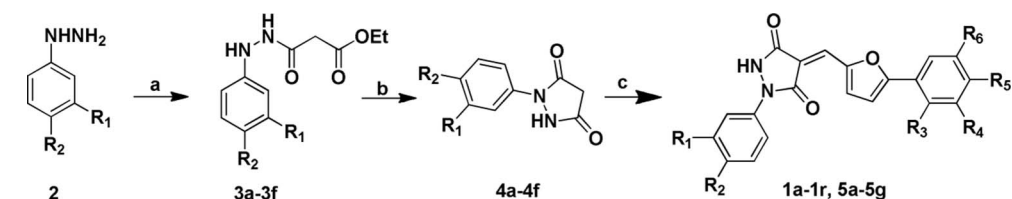
Binding modes of pyrazolidine-3,5-dione derivatives to c-Met kinase

To explore the binding modes of the derivatives to c-Met kinase, a molecular docking method was performed on the 18 compounds (**1a–r**). The results revealed that the compounds displayed a bent "U-shaped" binding mode as inhibitors of type I, as shown in Fig. 2(a). It indicates that the pyrazolidine-3,5-dione core is sandwiched into a narrow cleft formed by the P-loop of the N-lobe and the activation loop of the C-lobe.

Taking compound **1a** for example, in the hinge region of c-Met kinase, the atom N2H and atom O of the 3-carbonyl of the pyrazolidine-3,5-dione ring H-bond with the backbone CO and NH of Met1160 respectively. The A ring partially forms a π-stacking interaction with the phenyl ring of Tyr1159, with the ester substituent for the R$_2$ group pointed to the solvent. Similarly, the D ring also partially forms π-stacking interaction with Tyr1230 in the activation loop. Meanwhile, the carboxyl substituent for the R$_6$ group H-bonds with the backbone CO of Tyr1230 and the backbone NH of Arg1086 respectively in the P-loop. In addition, residues Ile1084, Val1092, Ala1108 and Leu1157 of the N-lobe form a stable hydrophobic environment for the compound, as

422 | *Org. Biomol. Chem.*, 2012, **10**, 421–430

This journal is © The Royal Society of Chemistry 2012

Table 1 Chemical structures and c-Met kinase inhibitory activities of compounds (**1a–1r**)

No	R$_1$	R$_2$	R$_3$	R$_4$	R$_5$	R$_6$	Inhibition (%)	IC$_{50}$ (μM)
1a	H	COOCH$_3$	H	H	Cl	COOH	49.3	9.5
1b*	H	COOCH$_3$	H	H	H	COOH	42.2	
1c*	H	COOEt	H	H	H	COOH	63.1	6.5
1d	H	CH$_3$	H	H	Cl	COOEt	48.1	
1e	H	CH$_3$	H	H	Cl	COOCH$_3$	56.8	7.8
1f*	H	OCH$_3$	H	H	F	COOH	23.6	
1g*	H	NO$_2$	H	H	F	COOH	43.2	
1h*	H	COOCH$_3$	CH$_3$	H	H	COOH	38.2	
1i*	H	COOEt	OCH$_3$	H	H	COOH	67.8	10.3
1j	CH$_3$	H	H	H	Cl	COOH	9.2	
1k	H	COOCH$_3$	H	H	H	Cl	21.0	
1l	H	COOCH$_3$	CH$_3$	Cl	H	H	35.6	
1m	H	COOCH$_3$	H	H	SO$_2$NH$_2$	H	56.2	10.4
1n	H	CH$_3$	H	H	(thiazol-2-yl)SO$_2$NH	H	43.4	
1o	Cl	CH$_3$	H	H	(thiazol-2-yl)SO$_2$NH	H	57.6	9.1
1p*	(structure)						42.2	
1q*	(structure)						6.8	
1r*	(structure)						8.0	

Scheme 1 Reagents and conditions: a) ethyl malonyl chloride, Et$_3$N, CH$_2$Cl$_2$; b) NaOH, EtOH; c) AcOH, reflux.

shown in Fig. 2(b). The binding mode analysis was quite in agreement with the SAR results aforementioned. By virtue of the key H-bond between the 3-carbonyl of the pyrazolidine-3,5-dione ring and the hinge region, the inhibitory activities were totally abolished when the 3-carbonyl was substituted. Since the substituent R$_2$ is pointed to the solvent and may form a van der Waal interaction with the backbone of the hinge region, the more hydrophilic groups such as esters and hydrophobic methyl are favored for the activities. The carboxyl group and ester group on R$_5$ or R$_6$ are likely to H-bond with the activation loop and P-loop, which in turn explains why the H-bond donors or acceptors are favored here.

As triazolopyridazines were reported to be the potent, selective, ATP-competitive inhibitors of c-Met kinase,[15] the binding modes were compared with compound **1a**. (Fig. 2(c)). The alignment shows that instead of the quinoline in the hinge region, compound
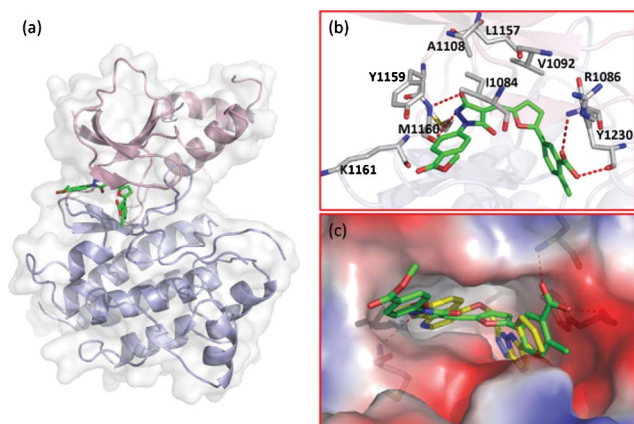
This journal is © The Royal Society of Chemistry 2012

Org. Biomol. Chem., 2012, **10**, 421–430 | 423

Fig. 2 Binding mode analysis of compound **1a** with c-Met kinase. (a) c-Met kinase is shown in cartoon, with the N-lobe shown in pink, while the C-lobe shown in purple. Compound **1a** occupies the ATP pocket between the two lobes and is shown in green sticks. (b) Detailed interactions of compound **1a** with surrounding key residues were analyzed. Compound **1a** is shown in green sticks, while surrounding key residues are shown in gray sticks. (c) Compound **1a** and triazolopyridazine molecule (in yellow sticks) were compared in the ATP pocket. The kinase is shown in electrostatic surface (the color blue indicates the positive-charge, while red indicates negative-charged).

1a possesses the pyrazolidine-3,5-dione ring forming the key H-bonds. Intrigued by the triazolopyridazine forming a stable π-stacking interaction with Tyr1230, a hybrid structure containing

a pyrazolidine-3,5-dione ring and a triazolopyridazine would be a good design to be investigated.

Focused combinatorial library design

Based on the SAR and binding mode analysis for the pyrazolidine-3,5-dione derivatives, a focused combinatorial library was designed, with structural fragments extracted from the potent derivatives and reported inhibitors. The LD1.0 program[16] was used during the focused library design. The binding mode analysis aforementioned indicates that the pyrazolidine-3,5-dione analogues can be divided into four parts. As shown in Fig. 3(a): part A is pointed into the solvent (site A), part B H-bonds with the hinge region (site B), part C is a linker between part A and B, probably forming π-stacking interaction with Tyr1230 if the length and orientation are reasonable, and the last part D is probably an aromatic ring with substituents H-bonding with the activation loop and P-loop. The LD1.0 program optimized 9 fragments for part A, 2 fragments for part B, 5 fragments for linker part C and 8 fragments for part D. The chemical structures of the fragments are shown in Fig. 3(b). Amongst them, fragments A1–A4 were designed with ester and methyl substituents on the benzyl ring aforementioned. As the hydrophilic substituents pointed into the solvent this probably make the compounds in the correct orientation. Fragments A5–A9 were designed based on the reported inhibitors, which proved to be favored for potent activity. Fragments B1–B2 were designed with the atom N2H and 3-carbonyl in the ring retained, which form H-bonds with
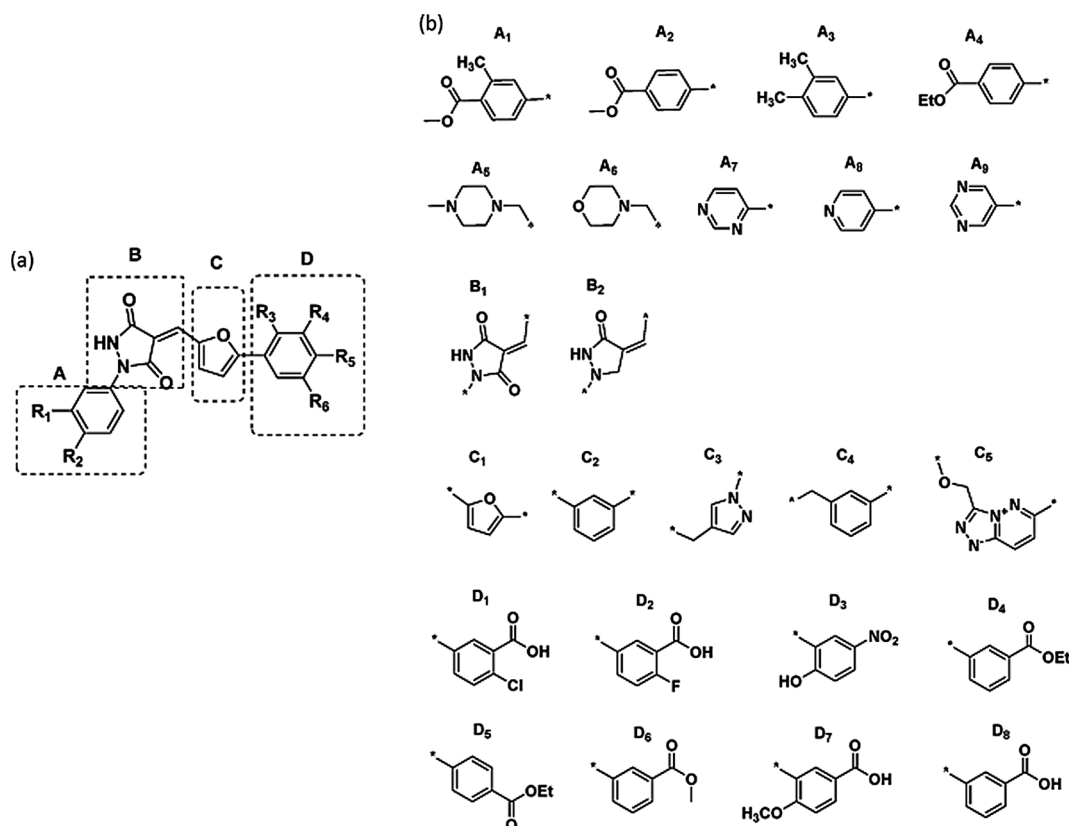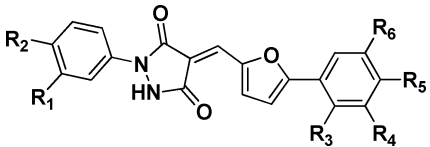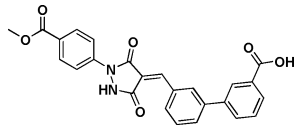

Fig. 3 (a) The pyrazolidine-3,5-dione scaffold was divided into four parts (A-B-C-D). (b) Building blocks for focused library generation. Fragments for parts A, B, C and D. The symbol * represents the site where fragments connect to each other to form a complete structure.

Table 2 Chemical structures and c-Met kinase inhibitory activities of 7 compounds selected from the focused library

No	Compound R_1	R_2	R_3	R_4	R_5	R_6	Inhibition (%)	IC$_{50}$ (μM)
5a[*]	H	COOCH$_3$	H	H	F	COOH	49.2	
5b	CH$_3$	CH$_3$	OH	H	H	NO$_2$	92.1	0.46
5c	H	COOCH$_3$	H	H	COOEt	H	74.2	0.91
5d	CH$_3$	CH$_3$	H	H	H	COOCH$_3$	48.2	
5e[*]	H	COOCH$_3$	OCH$_3$	H	H	COOH	75.2	6.9
5f[*]	H	COOEt	H	H	F	COOH	81.8	7.5
5g[*]							48.6	

the hinge region of the kinase. Different aromatic rings were designed for the linker part C, especially for the fragments C5 which was extracted from the X-ray structure. As for part D, different H-bonds donors and acceptors were tried on the benzyl ring, which were expected to H-bond with the activation loop and P-loop.

Then LD1.0 connected these fragments together according to sort A-B-C-D, producing a library containing 720 (9 × 2 × 5 × 8) molecules. All molecules in the designed library were first filtered by the drug-likeness of LD1.0, and then ranked by the scoring function of DOCK4.0,[17] AutoDock3.0.5[18,19] As AutoDock3.0.5 has a better ability to optimize binding poses as well as predicting binding energy. Besides the binding energy prediction by the score functions aforementioned, the ADMET properties and the favorable shape complementarity and potential in forming H-bonds with c-Met kinase were also analyzed.

The binding mode analysis aforementioned indicated that part A was pointed to the solvent flanked by the side-chain of residue Tyr1159 and residue Lys1161 (site A). Among these fragments, the morpholine group, which appears to serve as a solubilizing group and forms no ligand–protein interactions, was extracted from the reported inhibitor AM7 (PDB ID code: 2RFN).[20] Part B resides in the adenine site surrounded by residues Ile1084, Val1092, Ala1108 and Met1160 (site B), and the backbone of Met1160 anticipates the key H-bonds with compounds. The linker part C resides in the site C lined by residues Leu1140, Leu1157, Met1211, Ala1221, Asp1222, Ala1226 and Tyr1230. Considering the hydrophobic characteristic and potential for forming H-bond and π-stacking interactions, fragment C5 has an advantage. While, part D probably H-bonds with the residues Arg1086 in the P-loop, Asp1164, Asn1167, Arg1208, Asn1209, and Tyr1230 and Asp1231 in the activation loop. Consequently, the carboxyl, ester, hydroxyl and nitro substituents were favored on the benzyl ring. Unfortunately, related target compounds with morpholine and pyridine in site A and triazolopyridazine in site C have not been afforded due difficulties synthesising the intermediate. Finally, 7

compounds (**5a–g**) were successfully synthesized for biological testing as shown in Table 2.

Structure–activity relationship (SAR) analysis

In vitro assay indicates that, seven compounds (**5a–5g**) in Table 2 showed good c-Met kinase inhibitory activity and the activity of the most potent one **5b** (0.46 μM) increased 20 fold. The results illustrated that the 3,4-dimethylbenzene group (A3) is the most optimized fragment for part A; a furan group (C1) is the optimized fragment compared with a benzene group (C2) for part C; Fragments for part D are structurally more diverse than fragments for part C and a 2-hydroxy-4-nitrophenyl group (D3) was indicated to be the most favorable. Nevertheless, the fragment triazolopyridazine predicted to be favored was not added to the pyrazolidine-3,5-dione ring by virtue of the unstable intermediates in synthesis. Accordingly, the building blocks for parts B and C are fixed at fragments B1 and C1 and the fragments for parts A an D are a little bit flexible. The reason underlying the structure–activity relationship can be addressed from the binding modes of c-Met kinase with the compounds, which displayed a bent "U-shaped" binding mode in the ATP site. The R_2 group of phenyl ring A was directed toward a solvent-exposed area, which provides an opportunity for the introduction of polar, water-solubilizing substituents. Meanwhile, hydrophobic substituents may also be favored through van der Waals interactions with the backbone of Lys1161 His1162 and Gly1163. The most potent compound **5b** incorporating methyl groups in ring A supported this view. Part B resides in the hinge region and the key H-bond interaction is formed between 3-carbonyl of pyrazolidine-3,5-dione ring and Met1160. The inhibitory activities were abolished when the 3-carbonyl was substituted. Compounds with H-bond donor or acceptor groups (carboxyl-group, ester-group, hydroxyl group) on R_5 and R_6 possess potent inhibitory activity due to forming an H-bond interaction with Arg1086 in the P-loop, Asp1164, Arg1208, and Tyr1230 and Asp1231 in the activation loop. Introduction of other groups here actually decreased the inhibitory activity.

Conclusion

The discovery of c-Met kinase inhibitors is now of special interest in the treatment of cancer. In the present study, a series of pyrazolidine-3,5-dione derivatives were designed and synthesized based on the hit compound **1a**. All the compounds were evaluated for their ability to inhibit enzymatic activity of c-Met kinase by *in vitro* assay. Through substructure similarity search against the SPECS database and chemical synthesis methods, 4 compounds (**1c**, **1e**, **1m** and **1o**) tested by the enzyme-based assay against c-Met kinase showed potential inhibitory activity, with IC_{50} values mostly less than 10 μM. Based on the rich information of structure–activity relationship (SAR) and binding mode analysis, a focused combinatorial library was designed employing the LD1.0 program. Finally, seven compounds (**5a–g**) were proved to be potent inhibitors through *in vitro* assay. The activity of the most potent compounds **5b** ($IC_{50} = 0.46$ μM) was more than 20 times higher than that of the lead **1a**. Although, the theoretically favored fragments, such as morpholine, pyridine and triazolopyridazine, were not incorporated in our compounds, the pyrazolidine-3,5-dione is no doubt an optimized scaffold as inhibitor against c-Met kinase. Taking into account the rigid characteristic, further optimization of introducing alkyl with heteroatoms between the four parts and searching for other favored rings for the A and C parts, are still under way. Overall, the potent compounds discovered in this study demonstrated the feasibility for pyrazolidine-3,5-dione derivatives as c-Met kinase inhibitors and the efficiency of the strategy for the inhibitor design.

Experimental

Computational details

Molecular docking by DOCK4.0. To explore the detailed interactions of pyrazolidine-3,5-dione derivatives with c-Met kinase, the docking programs DOCK4.0[17] and AutoDock3.0.5[18,19] were employed. We used DOCK4.0 as the primary screening tool targeting at the active site of the X-ray crystal structure of c-Met kinase (PDB entry: 3CD8)[15] complexed with triazolopyridazine. Residues around the inhibitor at a radius of 6 Å were isolated for the construction of the grid for docking screening. This radius was large enough to include all of the residues involved in compound binding. During the docking procedure, Kollman all-atom charges were assigned to the protein, while Geisterger–Hückel charges were assigned to the compounds. In the docking search, the conformational flexibilities of the compounds were considered. We used 50 configurations per ligand-binding cycle and 60 maximum anchor orientations in the anchor-first docking algorithm. All docked configurations were energy minimized by the use of 100 maximum iterations and 1 minimization cycle. Prior to screening the compounds in the designed library, we tested this docking protocol by screening a small molecule database that contained 1000 compounds that consisted of 24 known inhibitors[15,20–24] and 976 decoy molecules. The result that inhibitors mostly reside at the top-scoring rank proved the feasibility of the protocol. The same test method was performed on the protocol of AutoDock3.03.

Molecular docking by AutoDock3.0.5. The X-ray crystal structure of c-Met kinase (PDB entry: 3CD8[15]) was also used as the receptor model by the AutoDock program. The ligand was removed at first and the polar hydrogen atoms were added. The potential of the enzyme was assigned with Kollman united charge encoded in SYBYL software package. The molecular geometry of compounds was also modeled using the SYBYL assigned with Gasteiger–Hückel charge. Some of the torsion angles were defined, allowing the conformation search for compounds during the docking process. The Lamarckian genetic algorithm (LGA) was applied to deal with the protein–inhibitor interactions. A Solis and Wets local search was performed for the energy minimization on a user-specified proportion of the population. The docked structures of compounds were generated after a reasonable number of evaluations. The docking simulation protocol is listed as follows: First, a PDBQ file of the kinase was created. Atomic salvation parameters and fragmental volumes were assigned to the enzyme using the ADDSOL module. Second, the grid map with $80 \times 80 \times 80$ points and a spacing of 0.375 Å were calculated using the AutoGrid program to evaluate the binding energies between the inhibitors and the enzyme. The grid center was set at the active site position (43.566 36.747 37.807) and the affinity and electrostatic potential grids were calculated for each type of atom in the inhibitors. The energetic configuration of a particular inhibitor was found by tri-linear interpolation of affinity values and electrostatic interaction of the eight grid points around each atom of the inhibitor. Third, some important parameters for LGA calculations were reasonably setup according to requirements of the Amber force field and our problem. Thirty docking simulations were performed for each compound and conformations of multiple runs were then clustered with the root-mean-square deviation (RMSD) tolerance of 1.0 Å. Finally, the proper conformation and position compared with the complex structure was extracted from the optimized complex.

Chemistry

The reagents (chemicals) were purchased from Lancaster, Acros, and Shanghai Chemical Reagent Co. and used without further purification. Analytical thin-layer chromatography (TLC) was HSGF 254 (150–200 μm thickness; Yantai Huiyou Co., China). Nuclear magnetic resonance (NMR) spectroscopy was performed on a Bruker AMX-400 and AMX-300 NMR (IS as TMS). Chemical shifts were reported in parts per million (ppm, δ) downfield from tetramethylsilane. Proton coupling patterns were described as singlet (s), doublet (d), triplet (t), quartet (q), multiplet (m), and broad (br). Low- and high-resolution mass spectra (LRMS and HRMS) were given with electric, electrospray, and matrix-assisted laser desorption ionization (EI, ESI, and MALDI) produced by a Finnigan MAT-95, LCQ-DECA spectrometer and IonSpec 4.7 T. The purity of final compounds was assessed by the analytical HPLC method and found to be >95%. An Agilent 1100 series HPLC with an Agilent Zorbax Exlipse SB-C18 (25–4.6 mm, 5 μm particle sizes) reversed-phase column was used for analytical HPLC analyses. The elution buffer was an A/B gradient, where A = H_2O and B = CH_3OH.

Methyl 4-(3,5-dioxopyrazolidin-1-yl)benzoate 4a. 4-Hydrazino-methylbenzoate hydrochloride (9.2 mmol) was stirred for 15 min at room temperature in a mixture of 10% aqueous Na_2CO_3 solution (20 mL) and CH_2Cl_2(40 mL). The separated aqueous

426 | *Org. Biomol. Chem.*, 2012, **10**, 421–430

This journal is © The Royal Society of Chemistry 2012

solution was extracted with CH_2Cl_2. The combined organic phases were dried over Na_2SO_4, filtered and concentrated. The residue was dissolved in anhydrous THF (50 mL) and Et_3N (10.1 mmol) was added. The reaction mixture was cooled to –10 °C and a solution of ethyl malonyl chloride (9.4 mmol) in anhydrous THF (25 mL) was added dropwise. The reaction mixture was allowed to warm to room temperature and stirred overnight. The reaction mixture was diluted with H_2O (100 mL) and extracted with EtOAc. The combined organic phases were washed with H_2O, brine, dried over Na_2SO_4, filtered and concentrated to yield crude compound as a brown residue. The crude compound was dissolved in EtOH (100 mL) and ethanolic 1 N NaOH solution (18.3 mmol) was added. The reaction mixture was stirred for 30 min at room temperature. The reaction mixture was then acidified by addition of aqueous 1 N HCl. The precipitate formed was collected by filtration, washed with water, and dried on the sintered glass to yield **4a** as a white solid. Yield: 70.2%. ^{1}H NMR (300 Hz, DMSO-d_6): δ 8.01–7.89 (m, 2H), 7.83–7.79 (m, 2H), 3.83 (s, 3H), 3.67 (s, 2H).

Ethyl 4-(3,5-dioxopyrazolidin-1-yl)benzoate 4b. As described in the preparation of **4a**, **4b** was prepared from 4-hydrazino-ethylbenzoate hydrochloride in the same manner. Yield: 69.3%. ^{1}H NMR (300 Hz, DMSO-d_6): δ 8.26 (m, 1H), 7.49 (m, 1H), 7.74 (m, 1H), 7.56 (m, 1H), 4.36–4.31 (m, 2H), 3.87 (s, 2H), 1.36–1.23 (m, 3H).

1-(4-Methoxyphenyl)pyrazolidine-3,5-dione 4c. In the same manner as described in the preparation of **4a**, **4c** was prepared from (4-methoxyphenyl)hydrazine hydrochloride. Yield: 73.5%. ^{1}H NMR (300 Hz, DMSO-d_6): δ 8.02–7.98 (m, 2H), 7.83–7.79 (m, 2H), 3.83 (s, 3H), 3.67 (s, 2H).

1-(4-Nitrophenyl)pyrazolidine-3,5-dione 4d. In the same manner as described in the preparation of **4a**, **4d** was prepared from (4-nitrophenyl)hydrazine hydrochloride. Yield: 60.6%. ^{1}H NMR (300 Hz, DMSO-d_6): δ 8.86–8.74 (m, 2H), 8.25–8.13 (m, 2H), 3.72 (s, 2H).

Ethyl 4-(3-ethoxy-5-oxo-4,5-dihydro-1H-pyrazol-1-yl)benzoate 4e. To a solution of methyl 4-(3,5-dioxopyrazolidin-1-yl)benzoate (**4a**, 1 mmol) in ethanol was added concentrated H_2SO_4 drop wise. The resulting mixture was refluxed overnight. Solvent was evaporated. $NaHCO_3$ solution was added to the residue and the solution was extracted with EtOAc. The organic layer was dried over Na_2SO_4, filtrated and concentrated to give the desired compound **4e** as a yellow solid. Yield: 92.3%. ^{1}H NMR (300 Hz, DMSO-d_6): δ 8.02–7.99 (m, 2H), 7.94–7.92 (m, 2H), 4.37–4.30 (m, 2H), 4.26–4.21(m, 2H), 3.74 (s, 2H), 1.36–1.23 (m, 6H).

Methyl 4-(3-methyl-5-oxo-4,5-dihydro-1H-pyrazol-1-yl)benzoate 4f. In the same manner as described in the preparation of **4a**, **4f** was prepared from 3-oxobutanoic acid. Yield: 90.1%. ^{1}H NMR (300 Hz, DMSO-d_6): δ 8.02–7.99 (m, 2H), 7.94–7.92 (m, 2H), 3.84 (s, 3H), 3.72 (s, 2H), 2.12 (s, 3H).

2-Chloro-5-(5-((1-(4-(methoxycarbonyl)phenyl)-3,5-dioxopyrazolidin-4-ylidene)methyl)furan-2-yl)benzoic acid 1a. Mp 237–239 °C. HPLC: 100%, t_R = 1.428 min. ^{1}H NMR (DMSO-d_6) δ: 8.28–8.61 (m, 2H), 7.85–8.17 (m, 5H), 7.73 (d, J = 8.5 Hz, 2H),

7.62 (t, J = 3.0 Hz, 1H), 3.86 (s, 3H). EI-MS m/z 466 [M$^+$]. HRMS (EI) m/z calcd for $C_{23}H_{15}ClN_2O_7$ [M$^+$] 466.0568, found 466.0589.

3-(5-((1-(4-(Methoxycarbonyl)phenyl)-3,5-dioxopyrazolidin-4-ylidene)methyl)furan-2-yl)benzoic acid 1b. General procedures for the synthesis of target compounds. The intermediate **4a** (1 mmol) and 3-(5-formylfuran-2-yl)benzoic acid (1 mmol) were dissolved in glacial acetic acid (5 mL). The reaction mixture was refluxed for 3 h. The precipitate formed was collected by filtration, washed with water, and dried on the sintered glass to yield **1b** as a yellow solid. Yield: 78.6%. Mp 232–234 °C. HPLC: 100.00%, t_R = 1.562 min. ^{1}H NMR (DMSO-d_6) δ: 8.42–8.63 (m, 1H), 8.18–8.26 (m, 1H), 7.91–8.08 (m, 6H), 7.64–7.74 (m, 2H), 7.54–7.61 (m, 1H), 3.86 (s, 3H). EI-MS m/z 432 [M$^+$]. HRMS (EI) m/z calcd for $_{16}C_{23}H_{16}N_2O_7$ [M$^+$] 432.0958, found 432.0962.

3-(5-((1-(4-(Ethoxycarbonyl)phenyl)-3,5-dioxopyrazolidin-4-yl-idene)methyl)furan-2-yl)benzoic acid 1c. In the same manner as described in the preparation of **1b**, **1c** was prepared from **4b** and 3-(5-formylfuran-2-yl)benzoic acid. Yield: 72.1%. Mp 241–246 °C. HPLC: 98.22%, t_R = 1.125 min. ^{1}H NMR (DMSO-d_6) δ: 8.42–8.62 (m, 1H), 8.19–8.28 (m, 1H), 7.90–8.08 (m, 6H), 7.56–7.74 (m, 3H), 4.33 (q, J = 7.1 Hz, 2H), 1.34 (t, J = 7.1 Hz, 3H). EI-MS m/z 446 [M$^+$]. HRMS (EI) m/z calcd for $C_{24}H_{18}N_2O_7$ [M$^+$] 446.1114, found 446.1120.

Ethyl 2-chloro-5-(5-((3,5-dioxo-1-p-tolylpyrazolidin-4-ylidene)-methyl)furan-2-yl)benzoate 1d. Mp 212–216 °C. HPLC: 96.12%, t_R = 6.235 min. ^{1}H NMR (DMSO-d_6) δ: 8.38–8.53 (m, 1H), 8.31–8.37 (m, 1H), 8.14 (d, J = 8.5 Hz, 1H), 7.76 (d, J = 8.5 Hz, 1H), 7.54–7.72 (m, 4H), 7.26 (d, J = 8.1 Hz, 2H), 4.40 (q, J = 7.1 Hz, 2H), 2.26–2.37 (m, 3H), 1.38 (t, 3H). EI-MS m/z 450 [M$^+$]. HRMS (EI) m/z calcd for $C_{24}H_{19}ClN_2O_5$ [M$^+$] 450.0982, found 450.0986.

Methyl 2-chloro-5-(5-((3,5-dioxo-1-p-tolylpyrazolidin-4-yli-dene)methyl)furan-2-yl)benzoate 1e. Mp 228–231 °C. HPLC: 97.55%, t_R = 6.336 min. ^{1}H NMR (DMSO-d_6) δ: 8.49 (d, J = 3.5 Hz, 1H), 8.36 (br s, 1H), 8.06–8.19 (m, 1H), 7.76 (d, J = 8.5 Hz, 1H), 7.54–7.70 (m, 4H), 7.26 (d, J = 8.5 Hz, 2H), 3.93 (s, 3H), 2.32 (s, 3H). EI-MS m/z 436 [M$^+$]. HRMS (EI) m/z calcd for $C_{23}H_{17}ClN_2O_5$ [M$^+$] 436.0826, found 436.0829.

2-Fluoro-5-(5-((1-(4-methoxyphenyl)-3,5-dioxopyrazolidin-4-yli-dene)methyl)furan-2-yl)benzoic acid 1f. In the same manner as described in the preparation of **1b**, **1f** was prepared from **4c** and 2-fluoro-5-(5-formylfuran-2-yl)benzoic acid. Yield: 79.6%. Mp 221–225 °C. HPLC: 100.00%, t_R = 1.987 min. ^{1}H NMR (300 MHz, DMSO-d_6) δ: 7.65–7.74 (m, 3H), 7.44–7.59 (m, 3H), 7.34–7.43 (m, 2H), 6.82–7.01 (m, 2H), 3.98 (s, 3H). EI-MS m/z 422 [M$^+$]. HRMS (EI) m/z calcd for $C_{22}H_{15}FN_2O_6$ [M$^+$] 422.0914, found 422.0926.

2 - Fluoro - 5 - (5 - ((1 - (4 - nitrophenyl) - 3,5 - dioxopyrazolidin - 4 - ylidene)methyl)furan-2-yl)benzoic acid 1g. In the same manner as described in the preparation of **1b**, **1g** was prepared from **4d** and 2-fluoro-5-(5-formylfuran-2-yl)benzoic acid. Yield: 76.3%. Mp 198–201 °C. HPLC: 100.00%, t_R = 1.235 min. ^{1}H NMR (DMSO-d_6) δ: 8.24–8.51 (m, 4H), 8.01–8.21 (m, 3H), 7.65 (s, 1H), 7.38–7.53 (m, 2H). EI-MS m/z 437 [M$^+$]. HRMS (EI) m/z calcd for $C_{21}H_{12}FN_3O_7$ [M$^+$] 437.0659, found 437.0664.

3-(5-((1-(4-(Methoxycarbonyl)phenyl)-3,5-dioxopyrazolidin-4-ylidene)methyl)furan-2-yl)-4-methylbenzoic acid 1h. In the same manner as described in the preparation of **1b**, **1h** was prepared from **4a** and 3-(5-formylfuran-2-yl)-4-methylbenzoic acid. Yield: 74.4%. Mp 221–224 °C. HPLC: 100.00%, t_R = 1.637 min. ^{1}H NMR (DMSO-d$_6$) δ: 8.57 (d, J = 3.2 Hz, 1H), 7.89–8.10 (m, 4H), 7.85 (t, J = 6.6 Hz, 1H), 7.73 (d, J = 7.4 Hz, 1H), 7.55–7.64 (m, 1H), 7.36–7.46 (m, 1H), 7.24–7.33 (m, 1H), 3.87 (s, 3H), 2.61 (s, 3H). EI-MS m/z 446 [M$^+$]. HRMS (EI) m/z calcd for $C_{24}H_{18}N_2O_7$ [M$^+$] 446.1114, found 446.1121.

3-(5-((1-(4-(Ethoxycarbonyl)phenyl)-3,5-dioxopyrazolidin-4-ylidene)methyl)furan-2-yl)-4-methoxybenzoic acid 1i. In the same manner as described in the preparation of **1b**, **1i** was prepared from **4b** and 3-(5-formylfuran-2-yl)-4-methoxybenzoic acid. Yield: 78.2%. Mp 205–209 °C. HPLC: 97.46%, t_R = 1.542 min. ^{1}H NMR (DMSO-d$_6$) δ: 8.62–8.74 (m, 1H), 8.39–8.58 (m, 1H), 7.96–8.08 (m, 4H), 7.92 (d, J = 8.9 Hz, 1H), 7.75 (d, J = 3.9 Hz, 1H), 7.38–7.47 (m, 1H), 7.33 (d, J = 8.9 Hz, 1H), 4.32 (d, J = 7.1 Hz, 2H), 4.07 (s, 3H), 1.34 (t, 3H). EI-MS m/z 476 [M$^+$]. HRMS (EI) m/z calcd for $C_{25}H_{20}N_2O_8$ [M$^+$] 476.1220, found 476.1215.

2-Chloro-5-(5-((3,5-dioxo-1-(m-tolyl)pyrazolidin-4-ylidene)methyl)furan-2-yl)benzoic acid 1j. Mp 194-197 °C. HPLC: 100%, t_R = 1.723 min. ^{1}H NMR (DMSO-d$_6$) δ: 8.53 (d, J = 2.7 Hz, 1H), 8.29–8.36 (m, 1H), 8.05–8.12 (m, 1H), 7.67–7.79 (m, 2H), 7.46–7.64 (m, 3H), 7.33 (t, J = 7.8 Hz, 1H), 7.02 (d, J = 7.1 Hz, 1H), 2.35 (s, 3H). EI-MS m/z 422 [M$^+$]. HRMS (EI) m/z calcd for $C_{22}H_{15}ClN_2O_5$ [M$^+$] 422.0669, found 422.0652.

Methyl 4-(4-((5-(3-chlorophenyl)furan-2-yl)methylene)-3,5-dioxopyrazolidin-1-yl)benzoate 1k. Mp 196–199 °C. HPLC: 100%, t_R = 5.359 min. ^{1}H NMR (DMSO-d$_6$) δ: 8.28 (m, 1H), 8.13 (d, J = 4.6 Hz, 1H), 7.62–7.92 (m, 5H), 7.50 (d, J = 8.5 Hz, 2H), 7.35–7.43 (m, 1H). EI-MS m/z 422 HRMS (EI) m/z calcd for $C_{22}H_{15}ClN_2O_5$ [M$^+$] 422.0669, found 422.0675.

Methyl 4-(4-((5-(3-chloro-2-methylphenyl)furan-2-yl)methylene)-3,5-dioxopyrazolidin-1-yl)benzoate 1l. Mp 183–187 °C. HPLC: 95.26%, t_R = 5.369 min. ^{1}H NMR (DMSO-d$_6$) δ: 8.53 (d, J = 2.8 Hz, 1H), 8.01–8.13 (m, 3H), 7.84–8.01 (m, 3H), 7.67–7.75 (m, 1H), 7.54 (d, J = 7.4 Hz, 2H), 3.86 (s, 3H), 2.41 (s, 3H). EI-MS m/z 436 [M$^+$]. HRMS (EI) m/z calcd for $C_{23}H_{17}ClN_2O_5$ [M$^+$] 436.0826, found 436.0833.

Methyl 4-(3,5-dioxo-4-((5-(4-sulfamoylphenyl)furan-2-yl)methylene)pyrazolidin-1-yl)benzoate 1m. Mp 189–192 °C. HPLC: 100.00%, t_R = 1.023 min. ^{1}H NMR (DMSO-d$_6$) δ: 8.55 (d, J = 3.5 Hz, 1H), 8.18 (d, J = 8.1 Hz, 2H), 8.01–8.09 (m, 2H), 7.96 (dd, J = 8.5, 1.8 Hz, 4H), 7.72 (d, J = 11.0 Hz, 1H), 7.62 (t, J = 4.1 Hz, 1H), 7.52 (s, 2H), 3.86 (s, 3H). EI-MS m/z 467 [M$^+$]. HRMS (EI) m/z calcd for $C_{22}H_{17}SN_2O_7$ [M$^+$] 467.0787 found 467.0780.

4-(5-((3,5-Dioxo-1-p-tolylpyrazolidin-4-ylidene)methyl)furan-2-yl)-N-(thiazol-2-yl)benzenesulfonamide 1n. Mp 212–216 °C. HPLC: 95.29%, t_R = 1.365 min. ^{1}H NMR (DMSO-d$_6$) δ: 12.88 (br s, 3H), 8.54 (d, J = 3.2 Hz, 1H), 8.12 (dd, J = 8.3, 3.4 Hz, 3H), 7.93 (d, J = 8.1 Hz, 3H), 7.52–7.73 (m, 4H), 7.21–7.34 (m, 3H), 6.88 (d, 1H), 2.32 (s, 3H). EI-MS m/z 506 [M$^+$]. HRMS (EI) m/z calcd for $C_{24}H_{18}S_2N_4O_5$ [M$^+$] 506.0719 found 506.0725.

4-(5-((1-(3-Chloro-4-methylphenyl)-3,5-dioxopyrazolidin-4-ylidene)methyl)furan-2-yl)-N-(thiazol-2-yl)benzenesulfonamide 1o. Mp:240–241 °C. HPLC: 98.22%, t_R = 1.412 min. ^{1}H NMR (DMSO-d$_6$): δ 8.55–8.54 (m, 1H), 8.14–8.10 (m, 2H), 7.94–7.91 (m, 2H), 7.69–7.56 (m, 3H), 7.31–7.25 (m, 3H), 6.89–6.88 (m, 1H), 2.32 (s, 3H). EI-MS m/z 540 [M$^+$]. HRMS (EI) m/z calcd for $C_{24}H_{17}S_2N_4O_5Cl$ [M$^+$] 540.0329 found 540.0335.

3′-((1-(4-(Ethoxycarbonyl)phenyl)-3,5-dioxopyrazolidin-4-ylidene)methyl)biphenyl-3-carboxylic acid 1p. In the same manner as described in the preparation of **1b**, **1p** was prepared from **4b** and 3′-formyl-[1,1′-biphenyl]-3-carboxylic acid. Yield: 77.3%. Mp 203–206 °C. HPLC: 100.00%, t_R = 1.725 min. ^{1}H NMR (DMSO-d$_6$) δ: 8.33 (d, J = 1.8 Hz, 1H), 8.20–8.42 (m, 1H), 7.85–8.17 (m, 7H), 7.55–7.86 (m, 4H), 7.28–7.51 (m, 1H), 4.29–4.33 (m, 2H), 1.30–1.34 (m, 3H). EI-MS m/z 456[M$^+$]. HRMS (EI) m/z calcd for $C_{26}H_{20}N_2O_6$ [M$^+$] 456.1321, found 456.1327.

3′-((3-Ethoxy-1-(4-(ethoxycarbonyl)phenyl)-5-oxo-1H-pyrazol-4(5H)-ylidene)methyl)biphenyl-3-carboxylic acid 1q. In the same manner as described in the preparation of **1b**, **1q** was prepared from **4e** and 3′-formyl-[1,1′-biphenyl]-3-carboxylic acid. Yield: 62.5%. Mp 211–214 °C. HPLC: 97.36%, t_R = 1.685 min. ^{1}H NMR (DMSO-d$_6$) δ: 8.58–8.68 (m, 1H), 8.32 (d, J = 12.0 Hz, 1H), 7.89–8.17 (m, 9H), 7.59–7.71 (m, 2H), 4.45–4.59 (m, 2H), 4.29–4.37 (m, 2H), 1.35 (d, J = 7.4 Hz, 6H). EI-MS m/z 484 [M$^+$]. HRMS (EI) m/z calcd for $C_{28}H_{24}N_2O_6$ [M$^+$] 484.1634 found 484.1639.

3-(5-((1-(4-(Methoxycarbonyl)phenyl)-3-methyl-5-oxo-1H-pyrazol-4(5H)-ylidene)methyl)furan-2-yl)benzoic acid 1r. In the same manner as described in the preparation of **1b**, **1r** was prepared from **4f** and 3-(5-formylfuran-2-yl)benzoic acid. Yield: 68.6%. Mp 221–225 °C. HPLC: 100.00%, t_R = 1.632 min. ^{1}H NMR (DMSO-d$_6$): δ 8.66–8.65 (m, 1H), 8.27 (s, 1H), 8.16–8.03 (m, 6H), 7.83 (s, 1H), 7.70–7.58 (m, 3H), 2.37 (s, 3H). EI-MS m/z 430 [M$^+$]. HRMS (EI) m/z calcd for $C_{24}H_{18}N_2O_6$ [M$^+$] 430.1165 found 430.1171.

2-Fluoro-5-(5-((1-(4-(methoxycarbonyl)phenyl)-3,5-dioxopyrazolidin-4-ylidene)methyl)furan-2-yl)benzoic acid 5a. In the same manner as described in the preparation of **1b**, **5a** was prepared from **4a** and 2-fluoro-5-(5-formylfuran-2-yl)benzoic acid. Yield: 73.9%. Mp 209–212 °C. HPLC: 100.00%, t_R = 1.874 min. ^{1}H NMR (DMSO-d$_6$) δ: 8.50–8.63 (m, 1H), 8.42 (d, J = 6.7 Hz, 1H), 8.16–8.26 (m, 1H), 7.99–8.07 (m, 3H), 7.88–7.99 (m, 1H), 7.71 (d, J = 2.8 Hz, 1H), 7.41–7.58 (m, 2H), 3.86 (s, 3H). EI-MS m/z 450[M$^+$]. HRMS (EI) m/z calcd for $C_{23}H_{15}FN_2O_7$ [M$^+$] 450.0863, found 450.0871.

1-(3,4-Dimethylphenyl)-4-((5-(5-hydroxy-2-nitrophenyl)furan-2-yl)methylene)pyrazolidine-3,5-dione 5b. Mp:274-278 °C. HPLC: 95.13%, t_R = 1.123 min. ^{1}H NMR (DMSO-d$_6$): δ 8.91–8.87 (m, 1H), 8.264 (s, 1H), 8.22–8.19 (m, 1H), 7.77–7.45 (m, 4H), 7.22–7.19 (m, 2H), 2.28 (s, 3H), 2.24 (s, 3H).; EI-MS m/z 419 [M$^+$]. HRMS (EI) m/z calcd for $C_{22}H_{17}N_3O_6$ [M$^+$] 419.1117 found 419.1125.

Ethyl 4-(5-((1-(4-(methoxycarbonyl)phenyl)-3,5-dioxopyrazolidin-4-ylidene)methyl)furan-2-yl)benzoate 5c. Mp 195–197 °C. HPLC:95.96%, t_R = 5.892. ^{1}H NMR (DMSO-d$_6$) δ: 8.53 (d, J = 3.5 Hz, 1H), 7.99–8.17 (m, 5H), 7.79–8.00 (m, 3H), 7.69 (d, J = 9.9 Hz, 1H), 7.62 (t, J = 3.7 Hz, 1H), 4.35 (q, J = 7.1 Hz, 2H), 3.86 (s, 3H), 1.35 (t, J = 7.1 Hz, 3H). EI-MS m/z 460 [M$^+$]. HRMS (EI) m/z calcd for $C_{25}H_{20}N_2O_7$ [M$^+$] 460.1271 found 460.1278.

Methyl 3-(5-((1-(3,4-dimethylphenyl)-3,5-dioxopyrazolidin-4-ylidene)methyl)furan-2-yl)benzoate 5d. Mp 204–207 °C. HPLC: 96.23%, t_R = 5.356 min. ^{1}H NMR (DMSO-d_6) δ: 8.42–8.59 (m, 2H), 8.25 (br. s., 1H), 8.03 (d, J = 7.8 Hz, 1H), 7.66–7.76 (m, 2H), 7.41–7.64 (m, 3H), 7.21 (d, J = 8.1 Hz, 1H), 3.93 (s, 3H), 2.27 (s, 3H), 2.23 (s, 3H). EI-MS m/z 416 [M$^+$]. HRMS (EI) m/z calcd for $C_{24}H_{20}N_2O_5$ [M$^+$] 416.1372 found 416.1378.

4-Methoxy-3-(5-((1-(4-(methoxycarbonyl)phenyl)-3,5-dioxopyrazolidin-4-ylidene)methyl)furan-2-yl)benzoic acid 5e. In the same manner as described in the preparation of **1b**, **5e** was prepared from **4a** and 3-(5-formylfuran-2-yl)-4-methoxybenzoic acid. Yield: 78.8%. Mp 216–219 °C. HPLC: 100.00%, t_R = 1.215 min. ^{1}H NMR (DMSO-d_6) δ: 8.66 (d, J = 8.5 Hz, 1H), 8.43–8.57 (m, 1H), 8.03 (s, 4H), 7.90–7.99 (m, 1H), 7.72 (s, 1H), 7.29–7.42 (m, 2H), 4.07 (s, 3H), 3.87 (s, 3H). EI-MS m/z 462 [M$^+$]. HRMS (EI) m/z calcd for $C_{24}H_{18}N_2O_8$ [M$^+$] 462.1063 found 462.1071.

5-(5-((1-(4-(Ethoxycarbonyl)phenyl)-3,5-dioxopyrazolidin-4-ylidene)methyl)furan-2-yl)-2-fluorobenzoic acid 5f. In the same manner as described in the preparation of **1b**, **5f** was prepared from **4b** and 2-fluoro-5-(5-formylfuran-2-yl)benzoic acid. Yield: 62.8%. Mp 212–214 °C. HPLC: 100.00%, t_R = 1.921 min. ^{1}H NMR (DMSO-d_6) δ: 8.25–8.55 (m, 2H), 7.93–8.11 (m, 4H), 7.85–7.92 (m, 1H), 7.69 (d, J = 7.3 Hz, 2H), 7.52–7.61 (m, 1H), 4.30 (q, J = 6.8 Hz, 2H), 1.32 (t, J = 7.1 Hz, 3H). EI-MS m/z 464 [M$^+$]. HRMS (EI) m/z calcd for $C_{24}H_{17}FN_2O_7$ [M$^+$] 464.1020 found 464.1027.

3′-((1-(4-(Methoxycarbonyl)phenyl)-3,5-dioxopyrazolidin-4-ylidene)methyl)biphenyl-3-carboxylic acid 5g. In the same manner as described in the preparation of **1b**, **5g** was prepared from **4a** and 3′-formyl-[1,1′-biphenyl]-3-carboxylic acid. Yield: 65.3%. Mp: 214–215 °C. HPLC: 99.15%, t_R = 1.326 min. ^{1}H NMR (DMSO-d_6) δ: 8.87–9.03 (m, 1H), 8.43–8.62 (m, 1H), 8.32 (s, 1H), 7.86–8.12 (m, 8H), 7.60–7.73 (m, 2H), 3.85 (m, 3H); EI-MS m/z 442 [M$^+$]. HRMS (EI) m/z calcd for $C_{25}H_{18}N_2O_6$ [M$^+$] 442.1165 found 442.1171.

ELISA kinase assay

The tyrosine kinase activities were evaluated according to the reported protocol.[25] Briefly, in enzyme-linked-immunosorbent assay (ELISA), 20 μg ml^{-1} Poly(Glu,Tyr)4 : 1 (Sigma) was pre-coated as a substrate in 96-well plates. 50 μl of 10 μM ATP solution diluted in kinase reaction buffer (50 mM HEPES pH 7.4, 50 mM MgCl$_2$, 0.5 mM MnCl$_2$, 0.2 mM Na$_3$VO$_4$, 1mM DTT) was added to each well. Various concentrations of compounds diluted in 10 μl of 1% DMSO (v/v) were added to each reaction well, with 1% DMSO (v/v) used as the negative control. The kinase reaction was initiated by the addition of purified c-Met kinase proteins diluted in 40 μl of kinase reaction buffer solution. After incubation for 60 min at 37 °C, the plate was washed three times with Phosphate Buffered Saline (PBS) containing 0.1% Tween 20 (T-PBS). Next, 100 μl anti-phosphotyrosine (PY99) antibody (1 : 500 diluted in 5 mg ml^{-1} BSA T-PBS) was added. After 30 min incubation at 37 °C, the plate was washed three times. 100 μl horseradish peroxidase-conjugated goat anti-mouse IgG (1 : 2000 diluted in 5 mg ml^{-1} BSA T-PBS) was added. The plate was reincubated at 37 °C for 30 min, and washed as before. Finally, 100 μl of a solution containing

0.03% H$_2$O$_2$ and 2 mg ml^{-1} *o*-phenylenediamine in 0.1 M citrate buffer, pH 5.5, was added and samples were incubated at room temperature until color emerged. The reaction was terminated by the addition of 50 μl of 2 M H$_2$SO$_4$, and the plate was read using a multiwell spectrophotometer (VERSAmax™, Molecular Devices, Sunnyvale, CA, USA) at 490 nm. The inhibition rate (%) was calculated using the following equation: [1 − ($A490$/$A490$ control)] × 100%. IC$_{50}$ values were calculated from the inhibition curves.

References

1 T. L. Underiner, T. Herbertz and S. J. Miknyoczki, *Anticancer Agents Med. Chem.*, 2010, **10**, 7.
2 P. M. Comoglio, S. Giordano and L. Trusolino, *Nat. Rev. Drug Discovery*, 2008, **7**, 504.
3 P. G. Dharmawardana, A. Giubellino and D. P. Bottaro, *Curr. Mol. Med.*, 2004, **4**, 855.
4 C. Birchmeier, W. Birchmeier, E. Gherardi and G. F. Vande Woude, *Nat. Rev. Mol. Cell Biol.*, 2003, **4**, 915.
5 F. Cecchi, D. C. Rabe and D. P. Bottaro, *Eur. J. Cancer*, 2010, **46**, 1260.
6 I. Canadas, F. Rojo, M. Arumi-Uria, A. Rovira, J. Albanell and E. Arriola, *Clin. Transl. Oncol.*, 2010, **12**, 253.
7 S. Naran, X. Zhang and S. J. Hughes, *Expert Opin. Ther. Targets*, 2009, **13**, 569.
8 W. K. You and D. M. McDonald, *BMB Rep.*, 2008, **41**, 833.
9 Z. Liang, D. Zhang, J. Ai, L. Chen, H. Wang, X. Kong, M. Zheng, H. Liu, C. Luo, M. Geng, H. Jiang and K. Chen, *Bioorg. Med. Chem. Lett.*, 2011, **21**, 3749.
10 K. Matsumoto and T. Nakamura, *Front. Biosci.*, 2008, **13**, 1943.
11 K. Matsumoto and T. Nakamura, *Biochem. Biophys. Res. Commun.*, 2005, **333**, 316.
12 L. Du, J. Ai, D. Li, T. Zhu, Y. Wang, M. Knauer, T. Bruhn, H. Liu, M. Geng, Q. Gu and G. Bringmann, *Chem.–Eur. J.*, 2011, **17**, 1319.
13 J. Baselga, *Science*, 2006, **312**, 1175.
14 L. He, L. Zhang, X. Liu, X. Li, M. Zheng, H. Li, K. Yu, K. Chen, X. Shen, H. Jiang and H. Liu, *J. Med. Chem.*, 2009, **52**, 2465.
15 B. K. Albrecht, J. C. Harmange, D. Bauer, L. Berry, C. Bode, A. A. Boezio, A. Chen, D. Choquette, I. Dussault, C. Fridrich, S. Hirai, D. Hoffman, J. F. Larrow, P. Kaplan-Lefko, J. Lin, J. Lohman, A. M. Long, A. Moriguchi, A. O'Connor, M. H. Potashman, M. Reese, K. Rex, A. Siegmund, K. Shah, R. Shimanovich, S. K. Springer, Y. Teffera, Y. Yang, Y. Zhang and S. F. Bellon, *J. Med. Chem.*, 2008, **51**, 2879.
16 G. Chen, S. Zheng, X. Luo, J. Shen, W. Zhu, H. Liu, C. Gui, J. Zhang, M. Zheng, C. M. Puah, K. Chen and H. Jiang, *J. Comb. Chem.*, 2005, **7**, 398.
17 T. Ewing and I. Kuntz, *J. Comput. Chem.*, 1998, **18**, 1175.
18 D. S. Goodsell, G. M. Morris and A. J. Olson, *J. Mol. Recognit.*, 1996, **9**, 1.
19 O. V. Buzko, A. C. Bishop and K. M. Shokat, *J. Comput.-Aided Mol. Des.*, 2002, **16**, 113.
20 S. F. Bellon, P. Kaplan-Lefko, Y. Yang, Y. Zhang, J. Moriguchi, K. Rex, C. W. Johnson, P. E. Rose, A. M. Long, A. B. O'Connor, Y. Gu, A. Coxon, T. S. Kim, A. Tasker, T. L. Burgess and I. Dussault, *J. Biol. Chem.*, 2008, **283**, 2675.

This journal is © The Royal Society of Chemistry 2012

Org. Biomol. Chem., 2012, **10**, 421–430 | 429

21 G. M. Schroeder, X. T. Chen, D. K. Williams, D. S. Nirschl, Z. W. Cai, D. Wei, J. S. Tokarski, Y. An, J. Sack, Z. Chen, T. Huynh, W. Vaccaro, M. Poss, B. Wautlet, J. Gullo-Brown, K. Kellar, V. Manne, J. T. Hunt, T. W. Wong, L. J. Lombardo, J. Fargnoli and R. M. Borzilleri, *Bioorg. Med. Chem. Lett.*, 2008, **18**, 1945.

22 Z. W. Cai, D. Wei, G. M. Schroeder, L. A. Cornelius, K. Kim, X. T. Chen, R. J. Schmidt, D. K. Williams, J. S. Tokarski, Y. An, J. S. Sack, V. Manne, A. Kamath, Y. Zhang, P. Marathe, J. T. Hunt, L. J. Lombardo, J. Fargnoli and R. M. Borzilleri, *Bioorg. Med. Chem. Lett.*, 2008, **18**, 3224.

23 J. Porter, S. Lumb, F. Lecomte, J. Reuberson, A. Foley, M. Calmiano, K. le Riche, H. Edwards, J. Delgado, R. J. Franklin, J. M. Gascon-Simorte, A. Maloney, C. Meier and M. Batchelor, *Bioorg. Med. Chem. Lett.*, 2009, **19**, 397.

24 N. D. D'Angelo, S. F. Bellon, S. K. Booker, Y. Cheng, A. Coxon, C. Dominguez, I. Fellows, D. Hoffman, R. Hungate, P. Kaplan-Lefko, M. R. Lee, C. Li, L. Liu, E. Rainbeau, P. J. Reider, K. Rex, A. Siegmund, Y. Sun, A. S. Tasker, N. Xi, S. Xu, Y. Yang, Y. Zhang, T. L. Burgess, I. Dussault and T. S. Kim, *J. Med. Chem.*, 2008, **51**, 5766.

25 I. Posner, M. Engel and A. Levitzki, *J. Biol. Chem.*, 1992, **267**, 20638.